Journal of Computational and Applied Mathematics 236 (2012) 4537–4546

Contents lists available at SciVerse ScienceDirect

Journal of Computational and Applied Mathematics

journal homepage: www.elsevier.com/locate/cam

Convergence of the discontinuous finite volume method for elliptic problems with minimal regularity

Jiangguo Liu [a,*], Lin Mu [b], Xiu Ye [c], Rabeea Jari [b]

[a] Department of Mathematics, Colorado State University, Fort Collins, CO 80523-1874, USA

[b] Department of Applied Science, University of Arkansas at Little Rock, Little Rock, AR 72204, USA

[c] Department of Mathematics, University of Arkansas at Little Rock, Little Rock, AR 72204, USA

ARTICLE INFO

Article history:
Received 26 June 2011
Received in revised form 13 March 2012

MSC:
65N15
65N30

Keywords:
Convergence analysis
Discontinuous finite volume methods
Elliptic boundary value problems
Interface problems
Low regularity

ABSTRACT

This paper investigates convergence of the discontinuous finite volume method (DFVM) under minimal regularity assumptions on solutions of second order elliptic boundary value problems. Conventional analysis requires the solutions to be in Sobolev spaces H^{1+s}, $s > \frac{1}{2}$. Here we assume the solutions are in H^{1+s}, $s > 0$ and employ the techniques developed in Gudi (2010) [18,20] to derive error estimates in a mesh-dependent energy norm and the L_2-norm for DFVM. The theoretical estimates are illustrated by numerical results, which include problems with corner singularity and intersecting interfaces.

1. Introduction

Finite volume methods have been widely used in sciences and engineering, e.g., computational fluid mechanics and petroleum reservoir simulations [1,2]. The integral formulation of a finite volume scheme for a partial differential equation (PDE) is obtained by integrating the PDE over a control volume. The integral formulation represents generally the conservation of a quantity of interest, e.g., mass, momentum, or energy. Finite volume methods can be formulated in the finite difference framework, known as cell-centered methods, or in the Petrov–Galerkin framework, categorized as finite volume element methods. We refer to the monographs [3,4] for general presentations of these methods, and to the papers [5–9] (also references therein) for more details. Compared to the finite difference and finite element methods, finite volume methods are usually easier to implement and offer flexibility for handling complicated domain geometries. More importantly, the methods ensure local conservation, a highly desirable property in many applications.

Motivated by the discontinuous Galerkin finite element methods [10,11], the discontinuous finite volume methods have been developed for second order elliptic problems and Stokes flows [9,12]. DFVMs are element-oriented. They offer better locality and even easier implementation [13]. By utilizing a connection operator inspired by the Crouzeix–Raviart nonconforming P_1 element [14,9], DFVMs can be embedded in the framework of discontinuous Galerkin finite element methods (DGFEMs). This enables us to borrow the ideas and techniques in error analysis for DGFEMs.

However, many real world applications, e.g., interface problems [15] and Darcy's flows in porous media [1,16] admit solutions with low regularity. Note that the standard *a priori* error estimates for DGFEMs, FVMs, DFVMs all require additional

* Corresponding author. Tel.: +1 970 491 3067.
E-mail addresses: liu@math.colostate.edu (J. Liu), lxmu@ualr.edu (L. Mu), xxye@ualr.edu (X. Ye), rhjari@ualr.edu (R. Jari).

0377-0427/$ – see front matter © 2012 Elsevier B.V. All rights reserved.
doi:10.1016/j.cam.2012.05.009

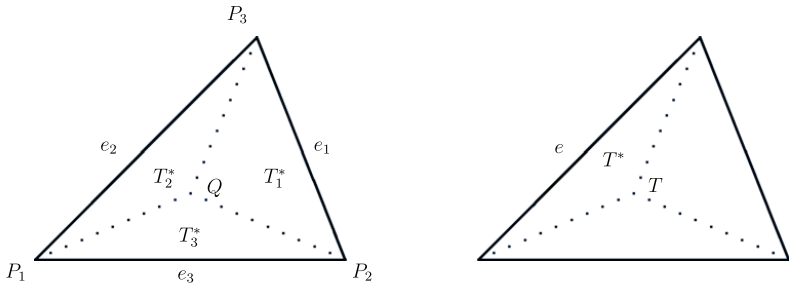

Fig. 1. A triangular element and its dual volumes.

regularity on the solutions. In particular, for second order elliptic problems, it is usually assumed [17,18] that the solutions are in H^{1+s}, $s > 1/2$. Recently there have been efforts on analyzing the DGFEM under low regularity of solutions. *A priori* error estimates in mesh-dependent energy norms are derived in [18] by applying new techniques that incorporate ideas usually seen in *a posteriori* analysis. Our recent work [19] presents an error estimate in the L_2-norm for DGFEMs for elliptic problems with low regularity solutions. Our analysis technique in [19] is based on the Raviart–Thomas interpolation operator and hence different (actually simpler) than that in [20]. Theoretical estimates and numerical results on DGFEMs for elliptic problems with solutions in $W^{2,p}$, $p < 2$ can be found in [21].

In this paper, we analyze the convergence of the DFVM for second order elliptic boundary value problems with minimal regularity assumptions on the solutions. Error estimates are derived in a mesh-dependent energy norm and the L_2-norm. The method is tested on problems with corner singularity and intersecting interfaces that indeed have solutions with very low regularity. The major contributions and novelty of this paper are reflected in the theoretical justification of DFVM's applications to low-regularity problems and the L_2-norm error analysis technique that are not seen in the literature yet.

The rest of this paper is organized as follows. In Section 2, we present the discontinuous finite volume formulation for elliptic problems. In Section 3, an optimal error estimate is derived in a mesh-dependent energy norm. An error estimate in the L_2-norm is also derived. In Section 4, we present numerical results to illustrate the theoretical estimates. These include a problem with corner singularity and another one with intersecting interfaces [15].

Throughout this paper, we use $A \lesssim B$ to represent $A \leq CB$ where C is an absolute constant independent of mesh sizes.

2. A discontinuous finite volume method for elliptic problems

We consider the following model elliptic boundary value problem

$$\begin{cases} \nabla \cdot (-\mathbf{K}\nabla u) = f & \text{in } \Omega, \\ u = 0 & \text{on } \partial\Omega, \end{cases} \tag{1}$$

where $\Omega \subset \mathbb{R}^2$ is a polygonal domain, $\mathbf{K}$ is a uniformly symmetric positive-definite permeability tensor. We shall develop a discontinuous finite volume method and analyze its performance under minimal regularity assumptions on the exact solution.

We adopt the standard definitions [22,9] for the Sobolev spaces $H^s(D)$ and their associated inner products $(\cdot,\cdot)_{s,D}$, norms $\|\cdot\|_{s,D}$, and seminorms $|\cdot|_{s,D}$ for $s \geq 0$. The space $H^0(D)$ coincides with $L_2(D)$, for which the norm and the inner product are denoted as $\|\cdot\|_D$ and $(\cdot,\cdot)_D$, respectively. If $D = \Omega$, we drop D.

Let $\mathcal{T}_h$ be a quasi-uniform triangulation of Ω. We define the dual partition $\mathcal{T}_h^*$ of $\mathcal{T}_h$ as follows. Each triangular element $T \in \mathcal{T}_h$ is divided into three triangles by connecting the barycenter and the three vertices of the triangle as shown in Fig. 1.

We define a finite dimensional space for trial functions associated with $\mathcal{T}_h$ as

$$V_h = \{v \in L_2(\Omega) : \ v|_T \in P_1(T), \ \forall T \in \mathcal{T}_h\} \tag{2}$$

and a finite dimensional space Q_h for piecewise constant test functions associated with the dual partition $\mathcal{T}_h^*$ as

$$Q_h = \{q \in L_2(\Omega) : \ q|_{T^*} \in P_0(T^*), \ \forall T^* \in \mathcal{T}_h^*\}, \tag{3}$$

where $P_k(T)$ (resp. $P_k(T^*)$) consists of all the polynomials defined on T (resp. T^*) with degree less than or equal to k.

Let $V(h) = V_h + H_0^1(\Omega)$. Define a mapping $I_h^* : V(h) \to Q_h$ by

$$(I_h^* v)|_{T^*} = \frac{1}{h_e} \int_e v|_{T^*} ds \quad \forall T^* \in \mathcal{T}_h^*, \tag{4}$$

as shown in Fig. 1, where h_e is the length of the edge e.

The following approximation properties of the operator I_h^* have been established in [6].

Lemma 2.1. *For any $v \in V_h$, we have*

$$\int_T (v - I_h^* v)dx = 0, \qquad \forall T \in \mathcal{T}_h, \tag{5}$$

$$\int_e (v - I_h^* v)ds = 0, \quad \forall e \in \partial T, \tag{6}$$

$$\|I_h^* w - w\|_{0,T} \le Ch_T |w|_{1,T}, \quad \forall T \in \mathcal{T}_h, \ \forall w \in V(h). \tag{7}$$

Let $\mathcal{E}_h$ denote the set of edges in $\mathcal{T}_h$ and $\mathcal{E}_h^0 := \mathcal{E}_h \setminus \partial\Omega$ the collection of all interior edges. Let e be an interior edge shared by two elements T_1 and T_2 in $\mathcal{T}_h$, and $\mathbf{n}_1$ and $\mathbf{n}_2$ be the unit normal vectors on e pointing to the exterior of T_1 and T_2, respectively. We define the average $\{\cdot\}$ and jump $[\cdot]$ on e for a scalar q and a vector $\mathbf{w}$ respectively as (see [10])

$$\{q\} = \frac{1}{2}(q|_{\partial T_1} + q|_{\partial T_2}), \qquad [q] = q|_{\partial T_1}\mathbf{n}_1 + q|_{\partial T_2}\mathbf{n}_2,$$

$$\{\mathbf{w}\} = \frac{1}{2}(\mathbf{w}|_{\partial T_1} + \mathbf{w}|_{\partial T_2}), \qquad [\mathbf{w}] = \mathbf{w}|_{\partial T_1} \cdot \mathbf{n}_1 + \mathbf{w}|_{\partial T_2} \cdot \mathbf{n}_2.$$

If e is a boundary edge on $\partial\Omega$, we define

$$\{q\} = q, \qquad [\mathbf{w}] = \mathbf{w} \cdot \mathbf{n}.$$

For convenience, we define

$$(v, w)_{\mathcal{T}_h} = \sum_{T\in\mathcal{T}_h} \int_T v\ w\ dx, \qquad (v, w)_{\mathcal{E}_h} = \sum_{e\in\mathcal{E}_h} \int_e v\ w\ ds.$$

Multiplying both sides of the elliptic equation in (1) by a test function $I_h^* v$, integrating by parts, summing over all finite volumes, and introducing penalty terms, we obtain a finite volume scheme as follows: seek $u_h \in V_h$ such that

$$A(u_h, v) = (f, I_h^* v), \quad \forall v \in V_h, \tag{8}$$

where $A(\cdot,\cdot)$ is a symmetric bilinear form defined as

$$A(u, v) = A_1(u, v) - (\{\mathbf{K}\nabla u\}, [I_h^* v])_{\mathcal{E}_h} - (\{\mathbf{K}\nabla v\}, [I_h^* u])_{\mathcal{E}_h} + (\alpha_e h_e^{-1}[I_h^* u], [I_h^* v])_{\mathcal{E}_h},$$

$$A_1(u, v) := -\sum_{T^*\in\mathcal{T}_h^*} \int_{\partial T^*} (\mathbf{K}\nabla u \cdot \mathbf{n})(I_h^* v)ds + \sum_{T\in\mathcal{T}_h} \int_{\partial T} (\mathbf{K}\nabla u \cdot \mathbf{n})(I_h^* v)ds,$$

and α_e is a penalty factor on edge e.

We further define a mesh-dependent norm $|||\cdot|||$ for $V(h)$ as follows

$$|||v|||^2 = \sum_{T\in\mathcal{T}_h} |v|_{1,T}^2 + \sum_{e\in\mathcal{E}_h} [I_h^* v]_e^2. \tag{9}$$

An equivalent mesh-dependent energy norm can be defined as

$$\|v\|_h^2 = \sum_{T\in\mathcal{T}_h} \left\|\mathbf{K}^{\frac{1}{2}}\nabla v\right\|_T^2 + \sum_{e\in\mathcal{E}_h} [I_h^* v]_e^2, \tag{10}$$

which involves the varying permeability $\mathbf{K}$.

The following trace inequality can be found in [17]. For any $w \in H^1(T)$ and any edge e of T, we have

$$\|w\|_e^2 \le C(h_e^{-1}|w|_T^2 + h_e|w|_{1,T}^2), \tag{11}$$

where C depends only on the minimum angle of T.

The following two lemmas have been established in [6]. Lemma 2.2 provides an equivalent formulation for the bilinear form $A_1(\cdot,\cdot)$, which will be used later in error analysis. Lemma 2.3 establishes the stability of the bilinear form $A(\cdot,\cdot)$, which requires the penalty factor α_e to be large enough. This usually depends on various factors, e.g., the quality of the triangular mesh (the minimal angles) and the permeability tensor.

Lemma 2.2. *For any $v, w \in V_h$, we have*

$$A_1(v, w) = (\mathbf{K}\nabla v, \nabla w)_{\mathcal{T}_h} + \sum_{T\in\mathcal{T}_h} \int_{\partial T} (I_h^* w - w)(\mathbf{K}\nabla v \cdot \mathbf{n})ds + \sum_{T\in\mathcal{T}_h} (\nabla \cdot \mathbf{K}\nabla v, w - I_h^* w)_T. \tag{12}$$

Lemma 2.3. *There exists a constant C independent of h such that the following holds for sufficiently large penalty factors α_e, $e \in \mathcal{E}_h$,*

$$A(v, v) \geq C|||v|||^2 \quad \forall v \in V_h. \tag{13}$$

3. Error estimation under minimal regularity assumptions

In this section, we present error estimates in the energy and L_2- norms. It is convenient and reasonable to assume that the permeability $\mathbf{K}$ is piecewise constant on $\mathcal{T}_h$. We start with a definition for data oscillations:

$$\mathrm{osc}(f)^2 = \sum_{T\in\mathcal{T}_h} h_T^2 \|f - f_T\|_T^2, \tag{14}$$

where f_T is the average of f on T.

As follows, Lemma 3.1 established in [23,24] allows us to approximate a discontinuous shape function in V_h by a continuous function v_I in $V_h \cap H_0^1(\Omega)$, which simplifies our error analysis. Lemma 3.2 established in [25] provides efficiency bounds for the *a posteriori* error estimates.

Lemma 3.1. *For any $v \in V_h$, there exists $v_I \in V_h \cap H_0^1(\Omega)$ such that*

$$\sum_{T\in\mathcal{T}_h} \left(\|v - v_I\|_T^2 + h_T^2 \|\nabla(v - v_I)\|_T^2\right) \lesssim \sum_{e\in\mathcal{E}_h} h_e \|[v]\|_e^2. \tag{15}$$

Lemma 3.2. *For any $v \in V_h$, $T \in \mathcal{T}_h$, and $e \in \mathcal{E}_h$, the following hold*

$$h_T \|f\|_T \lesssim \|\nabla(u - v)\|_T + h_T \|f - f_T\|_T,$$
$$h_e^{1/2} \|[\mathbf{K}\nabla v]\|_e \lesssim \|\nabla(u - v)\|_{\mathcal{T}_e} + h_T \|f - f_T\|_{\mathcal{T}_e},$$

where h_T is the diameter of the triangle T, h_e is the length of the edge e, and $\mathcal{T}_e$ is the union of the two triangles sharing the edge e.

Lemma 3.3. *Let $u \in H_0^1(\Omega)$ be the weak solution of (1) and $u_h \in V_h$ be the solution of (8), respectively. Then*

$$|||u - u_h||| \lesssim \inf_{v\in V_h} |||u - v||| + \mathrm{osc}(f). \tag{16}$$

Proof. For any $v \in V_h$, let $\phi = u_h - v$ and $\phi_I \in V_h \cap H_0^1(\Omega)$ satisfy (15). By (8) and Lemma 2.3, we have

$$\begin{aligned}
|||u_h - v|||^2 \lesssim\ & A(u_h - v, u_h - v) = A(u_h, \phi) - A(v, \phi) \\
\lesssim\ & (f, I_h^*\phi) - A(v, \phi - \phi_I) - A(v, \phi_I) \\
=\ & (f, I_h^*\phi - \phi) + (f, \phi - \phi_I) + (f, \phi_I) - A(v, \phi - \phi_I) - A(v, \phi_I) \\
=\ & (f, I_h^*\phi - \phi) + ((f, \phi - \phi_I) - A(v, \phi - \phi_I)) + ((f, \phi_I) - A(v, \phi_I)) \\
=:\ & I + II + III.
\end{aligned} \tag{17}$$

It follows from (5) and (7) that

$$I = (f, I_h^*\phi - \phi) = \sum_{T\in\mathcal{T}_h} (f - f_T, I_h^*\phi - \phi)_T \lesssim \mathrm{osc}(f)|||\phi|||. \tag{18}$$

Using the definition of $A(\cdot,\cdot)$, integration by parts, and Lemma 3.2, and the fact that $(\{\mathbf{K}\nabla v\}, [(\phi-\phi_I)-I_h^*(\phi-\phi_I)])_{\mathcal{E}_h} = 0$, we have

$$\begin{aligned}
II =\ & (f, \phi - \phi_I) - A(v, \phi - \phi_I) \\
=\ & (f, \phi - \phi_I) - (\mathbf{K}\nabla v, \nabla(\phi - \phi_I))_{\mathcal{T}_h} + (\{\mathbf{K}\nabla v\}, [I_h^*(\phi - \phi_I)])_{\mathcal{E}_h} \\
& + (\{\mathbf{K}\nabla(\phi - \phi_I)\}, [I_h^* v])_{\mathcal{E}_h} - (\alpha_e h_e^{-1} [I_h^* v], [I_h^*(\phi - \phi_I)])_{\mathcal{E}_h} \\
=\ & (f + \nabla\cdot\mathbf{K}\nabla v, \phi - \phi_I)_{\mathcal{T}_h} - ([\mathbf{K}\nabla v], \{\phi - \phi_I\})_{\mathcal{E}_h} \\
& + (\{\mathbf{K}\nabla(\phi - \phi_I)\}, [I_h^* v])_{\mathcal{E}_h} - (\alpha_e h_e^{-1} [I_h^*(u - v)], [I_h^*\phi])_{\mathcal{E}_h} \\
\lesssim\ & (|||u - v||| + \mathrm{osc}(f))|||\phi|||.
\end{aligned}$$

Since $\phi_I \in V_h \cap H_0^1(\Omega)$, it follows from the Cauchy–Schwarz inequality and the inverse estimate that

$$\begin{aligned} III &= (f, \phi_I) - A(v, \phi_I) \\ &= (\mathbf{K}\nabla u, \nabla\phi_I) - (\mathbf{K}\nabla v, \nabla\phi_I)_{\mathcal{T}_h} + (\{\mathbf{K}\nabla\phi\}, [I_h^* v])_{\mathcal{E}_h} \\ &= (\mathbf{K}\nabla(u-v), \nabla\phi_I)_{\mathcal{T}_h} - (\{\mathbf{K}\nabla\phi\}, [I_h^*(u-v)])_{\mathcal{E}_h} \\ &\lesssim |||u-v|||\,|||\phi|||. \end{aligned}$$

Combining the above estimates and (17), we obtain

$$|||u_h - v||| \lesssim |||u - v||| + \mathrm{osc}(f).$$

Finally, a triangle inequality leads to the desired estimate (16). □

The following theorem is an immediate result of Lemma 3.3.

Theorem 3.4. *Let $u \in H^{1+s}(\Omega)$, $s \in (0, 1]$ and $u_h \in V_h$ be the solutions of (1) and (8), respectively. Then*

$$|||u - u_h||| \lesssim h^s \|u\|_{1+s} + \mathrm{osc}(f). \tag{19}$$

Prior to furnishing an L_2-norm error estimate, we notice the following facts: for $v \in V_h \cap H_0^1(\Omega)$, it follows from (1) and (8) that

$$(\mathbf{K}\nabla u, \nabla v) = (f, v) \tag{20}$$

$$(\mathbf{K}\nabla u_h, \nabla v) = (f, I_h^* v) + (\{\mathbf{K}\nabla v\}, [I_h^* u_h])_{\mathcal{E}_h}. \tag{21}$$

The difference of the above two identities gives

$$(\mathbf{K}(\nabla u - \nabla u_h), \nabla v) = (f, v - I_h^* v) - (\{\mathbf{K}\nabla v\}, [I_h^* u_h])_{\mathcal{E}_h}. \tag{22}$$

Theorem 3.5. *Let $u \in H^{1+s}(\Omega)$, $s \in (0, 1]$ and $u_h \in V_h$ be the solutions of (1) and (8), respectively. Then*

$$\|u - u_h\| \lesssim h^{2s}\|u\|_{1+s} + h^{1+s}\|u\|_{1+s} + \mathrm{osc}(f). \tag{23}$$

Proof. Let $u_I \in V_h \cap H_0^1(\Omega)$ be an interpolant of u. Consider the dual problem

$$\begin{cases} \nabla\cdot(-\mathbf{K}\nabla w) = u_I - u_h & \text{in } \Omega, \\ w = 0 & \text{on } \partial\Omega. \end{cases} \tag{24}$$

It is assumed that for $s \in [0, 1]$, the following holds

$$\|w\|_{1+s} \lesssim \|u_I - u_h\|. \tag{25}$$

Denote $\phi = u_I - u_h$ and let $\phi_I \in V_h \cap H_0^1(\Omega)$ be an interpolant of ϕ satisfying (15). Testing (24) by $u_I - u_h$ gives

$$\begin{aligned} \|u_I - u_h\|^2 &= (\nabla\cdot(-\mathbf{K}\nabla w), u_I - u_h) = (\nabla\cdot(-\mathbf{K}\nabla w), \phi) \\ &= (\nabla\cdot(-\mathbf{K}\nabla w), \phi - \phi_I) + (\nabla\cdot(-\mathbf{K}\nabla w), \phi_I) \\ &= (\nabla\cdot(-\mathbf{K}\nabla w), \phi - \phi_I) + (\mathbf{K}\nabla w,\ \nabla\phi_I). \end{aligned} \tag{26}$$

Applying (15), (19), (24), and the Cauchy–Schwarz inequality leads to

$$\begin{aligned} |(\nabla\cdot(-\mathbf{K}\nabla w), \phi - \phi_I)| &\le \|\nabla\cdot(-\mathbf{K}\nabla w)\|\,\|\phi - \phi_I\| \lesssim h\|u_I - u_h\|\,|||\phi||| \\ &\lesssim h\|u_I - u_h\|(|||u - u_I||| + |||u - u_h|||) \\ &\lesssim h^{1+s}\|u\|_{1+s}\|u_I - u_h\|. \end{aligned} \tag{27}$$

Let $w_I \in V_h \cap H_0^1(\Omega)$ be an interpolant of w. The second term on the right hand side of (26) can be estimated as

$$\begin{aligned} (\mathbf{K}\nabla w, \nabla\phi_I) &= (\mathbf{K}(\nabla w - \nabla w_I), \nabla\phi_I) + (\mathbf{K}\nabla w_I, \nabla\phi_I) \\ &= (\mathbf{K}(\nabla w - \nabla w_I), \nabla\phi_I - \nabla\phi) + (\mathbf{K}(\nabla w - \nabla w_I), \nabla\phi) + (\mathbf{K}\nabla w_I, \nabla\phi_I) \\ &= (\mathbf{K}(\nabla w - \nabla w_I), \nabla\phi_I - \nabla\phi) + (\mathbf{K}(\nabla w - \nabla w_I), \nabla(u_I - u)) \\ &\quad + (\mathbf{K}(\nabla w - \nabla w_I), \nabla(u - u_h)) + (\mathbf{K}\nabla w_I, \nabla\phi_I). \end{aligned} \tag{28}$$

The fourth term above can be rewritten as

$$(\mathbf{K}\nabla w_I, \nabla\phi_I) = (\mathbf{K}\nabla w_I, \nabla\phi_I - \nabla\phi) + (\mathbf{K}\nabla w_I, \nabla\phi). \tag{29}$$

Recall that $\mathbf{K}$ is assumed to be piecewise constant and w_I is linear. Integration by parts yields

$$\begin{aligned}(\mathbf{K}\nabla w_I, \nabla\phi_I - \nabla\phi) &= -(\nabla\cdot(\mathbf{K}\nabla w_I), \phi - \phi_I)_{\mathcal{T}_h} + \sum_{T\in\mathcal{T}_h}(\mathbf{K}\nabla w_I\cdot\mathbf{n}, \phi_I - \phi)_{\partial T}\\ &= ([\mathbf{K}\nabla w_I], \{\phi_I - \phi\})_{\mathcal{E}_h^0} + (\{\mathbf{K}\nabla w_I\}, [u_h])_{\mathcal{E}_h}. \end{aligned} \tag{30}$$

It follows from (22) that

$$\begin{aligned}(\mathbf{K}\nabla w_I, \nabla\phi) &= (\mathbf{K}(\nabla u_I - \nabla u_h), \nabla w_I)\\ &= (\mathbf{K}(\nabla u_I - \nabla u), \nabla w_I) + (\mathbf{K}(\nabla u - \nabla u_h), \nabla w_I)\\ &= (\mathbf{K}(\nabla u_I - \nabla u), \nabla w_I - \nabla w) + (\mathbf{K}(\nabla u_I - \nabla u), \nabla w) + (f, w_I - I_h^* w_I) - (\{\mathbf{K}\nabla w_I\}, [I_h^* u_h])_{\mathcal{E}_h}. \end{aligned} \tag{31}$$

Note that w_I is linear and $\int_e (u_h - I_h^* u_h)ds = 0$ for any $e \in \mathcal{E}_h$. Combining the last terms on the right hand sides of (30) and (31) gives

$$(\{\mathbf{K}\nabla w_I\}, [u_h])_{\mathcal{E}_h} - (\{\mathbf{K}\nabla w_I\}, [I_h^* u_h])_{\mathcal{E}_h} = 0. \tag{32}$$

By (24), continuity of u and u_I and integration by parts, the second term in the right hand side of (31) becomes

$$(\mathbf{K}(\nabla u_I - \nabla u), \nabla w) = (\nabla\cdot(-\mathbf{K}\nabla w), u_I - u). \tag{33}$$

Combining (29)–(33) gives

$$\begin{aligned}(\mathbf{K}\nabla w_I, \nabla\phi_I) &= ([\mathbf{K}\nabla w_I], \{\phi_I - \phi\})_{\mathcal{E}_h^0} + (\mathbf{K}(\nabla u_I - \nabla u), \nabla w_I - \nabla w)\\ &\quad + (\nabla\cdot(-\mathbf{K}\nabla w), u_I - u) + (f - f_T, w_I - I_h^* w_I)_{\mathcal{T}_h}. \end{aligned}$$

Applying (15), (25), Lemma 3.2, and the definitions of u_I, w_I, we have

$$|(\mathbf{K}\nabla w_I, \nabla\phi_I)| \lesssim (h^{2s}\|u\|_{1+s} + h^{1+s}\|u\|_{1+s} + \mathrm{osc}(f))\|u_I - u_h\|. \tag{34}$$

Note that (28) and (34) together imply

$$|(\mathbf{K}\nabla w, \nabla\phi_I)| \lesssim (h^{2s}\|u\|_{1+s} + h^{1+s}\|u\|_{1+s} + \mathrm{osc}(f))\|u_I - u_h\|. \tag{35}$$

Combining (26), (27) and (35) leads to

$$\|u_I - u_h\| \lesssim h^{2s}\|u\|_{1+s} + h^{1+s}\|u\|_{1+s} + \mathrm{osc}(f).$$

The proof is completed by applying a triangle inequality. □

Remark 3.6. Let $u \in H^2(\Omega)$ (that is, $s = 1$), and $u_h \in V_h$ be respectively the solutions of (1) and (8). Then

$$\|u - u_h\| \lesssim h^2(\|u\|_2 + \|f\|_1). \tag{36}$$

The counterexamples in [7,26] show that the assumption of $f \in H^1(\Omega)$ is necessary for the finite volume methods to have optimal L^2-norm error estimates.

4. Numerical results

In this section, we conduct numerical experiments on two widely tested model problems.

Example 1 (*Corner Singularity*)**.** We first consider an example with a corner singularity that was also tested in [21]. Here $\Omega = (0, 1)^2$, the permeability $\mathbf{K}$ is just the 2×2 identity matrix $\mathbf{I}_2$, the exact solution is

$$u(x, y) = x(1 - x)y(1 - y)r^{-2+\gamma}, \tag{37}$$

where $r = \sqrt{x^2 + y^2}$ is the polar radius and $\gamma \in (0, 1]$ is a constant. Clearly, the exact solution admits a corner singularity at the origin. It can be verified [21] that $u \in W^{2,p}(\Omega)$ with

$$p = \frac{2}{2 - \gamma} + \delta$$

for any $\delta > 0$. By the Sobolev embedding theorem [22], we have

$$u \in H_0^1(\Omega) \cap H^{1+\gamma-\varepsilon}(\Omega), \qquad u \notin H^{1+\gamma}(\Omega),$$

where ε is any small positive number. For convenience, we set $s = \gamma - \varepsilon$.

Table 1
Example 1: Errors and convergence rates of DFVM solutions on uniform triangular meshes.

$1/h$	$\gamma = 1$		$\gamma = 0.25$		$\gamma = 0.0625$	
	$\|\|\|u - u_h\|\|\|$	$\|u - u_h\|$	$\|\|\|u - u_h\|\|\|$	$\|u - u_h\|$	$\|\|\|u - u_h\|\|\|$	$\|u - u_h\|$
16	3.8290E−2	6.2082E−4	5.5817E−1	1.3589E−2	1.2544E+0	3.9693E−2
20	3.1463E−2	4.0403E−4	5.2885E−1	1.0268E−2	1.2381E+0	3.1343E−2
24	2.6799E−2	2.8422E−4	5.0588E−1	8.1654E−3	1.2248E+0	2.5833E−2
28	2.3364E−2	2.1104E−4	4.8716E−1	6.7268E−3	1.2135E+0	2.1934E−2
32	2.0718E−2	1.6303E−4	4.7144E−1	5.6872E−3	1.2038E+0	1.9034E−2
36	1.8632E−2	1.2982E−4	4.5797E−1	4.9044E−3	1.1952E+0	1.6795E−2
40	1.6938E−2	1.0588E−4	4.4623E−1	4.2961E−3	1.1876E+0	1.5016E−2
44	1.5530E−2	8.8046E−5	4.3585E−1	3.8112E−3	1.1807E+0	1.3569E−2
48	1.4347E−2	7.4398E−5	4.2658E−1	3.4165E−3	1.1744E+0	1.2370E−2
52	1.3334E−2	6.3718E−5	4.1821E−1	3.0897E−3	1.1686E+0	1.1361E−2
56	1.2455E−2	5.5200E−5	4.1061E−1	2.8151E−3	1.1633E+0	1.0500E−2
60	1.1684E−2	4.8296E−5	4.0364E−1	2.5815E−3	1.1584E+0	9.7576E−3
64	1.1006E−2	4.2620E−5	3.9724E−1	2.3806E−3	1.1538E+0	9.1105E−3
$\mathcal{O}(h^s)$	0.9003	1.9329	0.2456	1.2567	0.0604	1.0620

Table 2
Example 1: Convergence rates for DFVM solutions on uniform triangular meshes.

γ	Conv. rate of $\|\|\|u - u_h\|\|\|$	Conv. rate of $\|u - u_h\|$
1	0.9003	1.9329
0.5	0.4916	1.5131
0.25	0.2456	1.2567
0.125	0.1231	1.1287
0.0625	0.0604	1.0620
0.03125	0.0269	1.0331

Tabulated in Tables 1 and 2 are the errors and convergence rates obtained by applying the DFVM on uniform triangular meshes. Linear regression is used to calculate the convergence rates. It is clear that the energy norm convergence rate is s, whereas the L_2-norm convergence rate is $1 + s$. As reflected in Theorem 3.5 and its proof, the L_2-norm convergence rate is mainly a balance of the two terms $\mathcal{O}(h^{2s})$ and $\mathcal{O}(h^{1+s})$, since $h^s\mathrm{osc}(f)$ is a higher order term. For particular problems like Example 1, it could be as good as $(1 + s)$.

In [21], DGFEMs with shape functions of piecewise polynomials with degree 1, 2, 3 are used on uniform triangular meshes. Similar conclusions regarding convergence rates in a mesh-dependent energy norm are reached. There is a statement about convergence rates in the L_2-norm, but no error results are presented.

One may notice that for the mesh-dependent energy norms, neither the convergence rates in [21] nor the rates in this paper reach exactly γ. They are a bit off. Similar phenomena can be observed for the L_2-norm convergence rates. This is mainly due to the fact that the exact solution $u \in H^{1+\gamma-\varepsilon}(\Omega)$ for any small positive ε, but $u \notin H^{1+\gamma}(\Omega)$. Utilizing Besov spaces [27], one can have a more accurate description

$$u \in B^{1+\gamma}_{2,\infty}(\Omega), \qquad u \notin B^{1+\gamma}_{2,q}(\Omega) \quad \text{for } q < \infty.$$

It is also known that

$$H^{1+\gamma} = B^{1+\gamma}_{2,2}, \qquad B^{1+\gamma}_{2,q}(\Omega) \subsetneq B^{1+\gamma}_{2,\infty}(\Omega) \quad \text{for } q < \infty.$$

However, there is no inner product structure in general Besov spaces and calculating Besov norms is very technical. Furthermore, the variational forms for (continuous and discontinuous Galerkin) finite element schemes are based upon the Riesz Representation Theorem, which relies on duality and the inner product structure.

Example 2 (*Intersecting Interfaces*)**.** This problem is derived from the one proposed in [15], which has been widely tested [28]. We have merely changed the sign of the exact solution in the original problem for viewing convenience. Consider $\Omega = (-1, 1)^2$ and the x-, y-axes as intersecting interfaces. The permeability is $K_1\mathbf{I}_2$ in the 1st and 3rd quadrants and $K_2\mathbf{I}_2$ in the 2nd and 4th quadrants. In the polar coordinates, the exact solution takes the form

$$u(x, y) = -r^\gamma \mu(\theta),$$

where $\gamma \in (0, 1]$ and

$$\mu(\theta) = \begin{cases} \cos((\pi/2 - \sigma)\gamma)\cos((\theta - \pi/2 + \rho)\gamma), & \text{if } 0 \le \theta \le \pi/2, \\ \cos(\rho\gamma)\cos((\theta - \pi + \sigma)\gamma), & \text{if } \pi/2 \le \theta \le \pi, \\ \cos(\sigma\gamma)\cos((\theta - \pi - \rho)\gamma), & \text{if } \pi \le \theta \le 3\pi/2, \\ \cos((\pi/2 - \rho)\gamma)\cos((\theta - 3\pi/2 - \sigma)\gamma), & \text{if } 3\pi/2 \le \theta \le 2\pi. \end{cases} \tag{38}$$

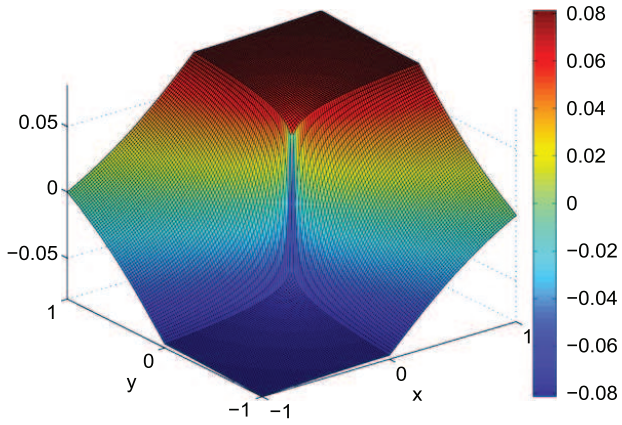

Fig. 2. Example 2: A plot of the exact solution.

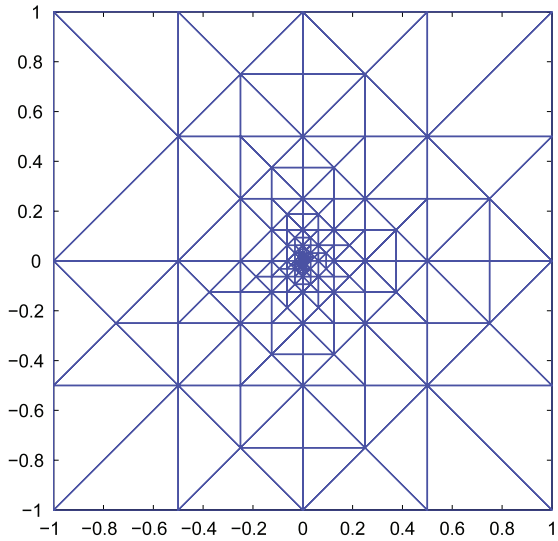

Fig. 3. Example 2: The initial triangular mesh used in the numerical experiments.

The parameters γ, ρ, σ satisfy the following nonlinear relations

$$\begin{aligned} &R := K_1/K_2 = -\tan((\pi/2-\sigma)\gamma)\cot(\rho\gamma),\\ &1/R = -\tan(\rho\gamma)\cot(\sigma\rho),\\ &R = -\tan(\rho\gamma)\cot((\pi/2-\rho)\gamma),\\ &\max\{0, \pi\gamma-\pi\} < 2\gamma\rho < \min\{\pi\gamma, \pi\},\\ &\max\{0, \pi-\pi\gamma\} < -2\gamma\sigma < \min\{\pi, 2\pi-\pi\gamma\}. \end{aligned} \tag{39}$$

The solution $u(r,\theta)$ is known to be in $H^{1+\gamma-\varepsilon}(\Omega)$ for any $\varepsilon > 0$. Again, if Besov spaces are used, then we have a more accurate characterization $u \in B^{1+\gamma}_{2,\infty}(\Omega)$. Shown in Fig. 2 is a plot of the exact solution that exhibits the intersecting sharp interfaces at the origin.

A widely tested case is $\gamma = 0.1$, $R \approx 161$, $\rho \approx \pi/4$, $\sigma \approx -14.922$.

To resolve the singularity induced by the intersecting interfaces, we start with a triangular mesh locally refined near the origin as shown in Fig. 3, which has 331 elements and 174 nodes. Then the mesh is uniformly refined by bisecting the longest edges, so that the mesh size is reduced from h to $h/\sqrt{2}$ for each refinement.

For Example 2, it can be observed from Table 3 that the energy-norm convergence rate is close to γ. By Theorem 3.4, the theoretical energy-norm convergence rate would be γ, since $f \equiv 0$ and $\mathrm{osc}(f) \equiv 0$. However, the L_2-norm convergence rate is better than 2γ. This is not a surprise, since Theorem 3.5 asserts that theoretically the error is a combination of $h^{1+\gamma}$ and $h^{2\gamma}$.

Shown in Table 4 are the errors measured in the equivalent mesh-dependent energy norm defined in (10). Note that this norm depends on the varying permeability. For Example 2, due to the large jump in the permeability, the results are not as good as those for the norm defined in (9), which does not involve the varying permeability.

Table 3
Example 2: Errors and convergence rates in the mesh-dependent energy and L_2-norms.

Mesh level	$\|\|\|u - u_h\|\|\|$	$\|u - u_h\|$
1	1.457485E−1	5.241524E−3
2	1.390240E−1	3.823979E−3
3	1.328554E−1	3.478748E−3
4	1.292828E−1	3.172465E−3
5	1.265692E−1	2.925122E−3
6	1.238210E−1	2.810386E−3
Conv. rate	0.09	0.33

Table 4
Example 2: Errors and convergence rate in an equivalent mesh-dependent energy norm.

Mesh level	$\|u - u_h\|_h$
1	2.698229E−1
2	2.646828E−1
3	2.544759E−1
4	2.488108E−1
5	2.390425E−1
6	2.366103E−1
Conv. rate	0.08120

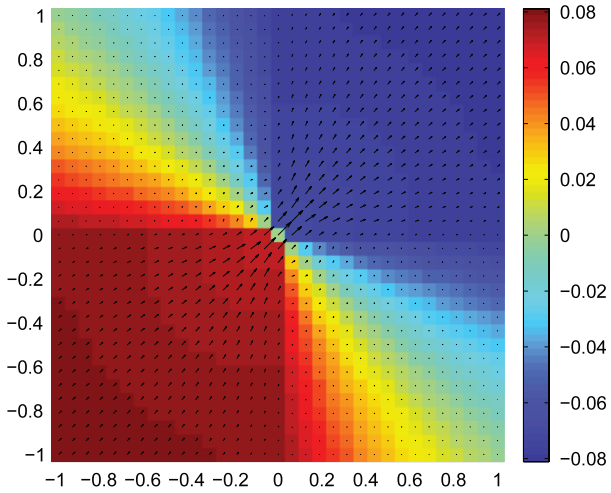

Fig. 4. Example 2: Pressure and velocity profiles for the DFVM numerical solution on a uniform triangular mesh with $h = 1/16$, if the intersecting interface problem is interpreted as a flow problem.

Example 2 can also be interpreted as a flow problem. Shown in Fig. 4 are the pressure and velocity profiles for the DFVM numerical solution on a uniform triangular mesh with $h = 1/16$. The flow is barely visible in the low permeability region consisting of the 2nd and 4th quadrants. The 1st and 3rd quadrants together form a region with a very high permeability. In this context, the x-, y-axes are permeability barriers. The flow runs from a high pressure domain (the 1st quadrant) to a low pressure domain (the 3rd quadrant), squeezing through the only pass at the origin.

5. Concluding remarks

For second order elliptic boundary value problems, the discontinuous finite volume method along with discontinuous Galerkin finite element methods can be formulated on the Sobolev space H^1. Convectional analysis techniques require the problems to have solutions with regularity H^{1+s}, $s > \frac{1}{2}$. Here in this paper, new techniques are used to analyze errors for problems with regularity H^{1+s}, $s \in (0, 1]$. The theoretical analysis justifies the applications of the DFVM to problems with low regularity, e.g., those with corner singularity or interior interfaces.

Darcy's flows in porous media represent another class of problems that possess low regularity [16,13,29]. Two salient features of Darcy's flows in porous media are (1) the permeability is discontinuous (usually piecewise constant); (2) no exact solution is known. These can be interpreted as elliptic interface problems also. It is recognized that the solutions have low regularity, but there is no general quantitative characterization of regularity of the solutions, as to the authors'

best knowledge. With the theoretical results in this paper, [21,30], applications of the DFVM and the DGFEM to Darcy's flows are justified. Quantifying regularity of Darcy's flows and calibrating the performance of the DFVM and the DGFEM on Darcy's flows should be interesting problems for further investigation.

Acknowledgments

X. Ye was supported in part by US National Science Foundation under Grant No. DMS-0813571. J. Liu thanks Pattern Analysis Laboratory at Colorado State University for use of their computing facilities for some computing tasks performed in this research paper.

References

[1] Z. Chen, G. Huan, Y. Ma, Computational Methods for Multiphase Flows in Porous Media, SIAM, 2006.
[2] R. Lazarov, I. Michev, P. Vassilevski, Finite volume methods for convection–diffusion problems, SIAM J. Numer. Anal. 33 (1996) 31–55.
[3] R. Eymard, T. Gallouët, R. Herbin, Finite Volume Methods: Handbook of Numerical Analysis, North-Holland, Amsterdam, 2000.
[4] R. Li, Z. Chen, W. Wu, Generalized Difference Methods for Differential Equations: Numerical Analysis of Finite Volume Methods, Marcel Dekker, New York, 2000.
[5] Z. Cai, J. Mandel, S. McCormick, The finite volume element method for diffusion equations on general triangulations, SIAM J. Numer. Anal. 28 (1991) 392–402.
[6] S. Chou, X. Ye, Unified analysis of finite volume methods for second order elliptic problems, SIAM J. Numer. Anal. 45 (2007) 1639–1653.
[7] R.E. Ewing, T. Lin, Y. Lin, On the accuracy of the finite volume element method based on piecewise linear polynomials, SIAM J. Numer. Anal. 39 (2002) 1865–1888.
[8] M. Yang, J. Liu, A quadratic finite volume element method for parabolic problems on quadrilateral meshes, IMA J. Numer. Anal. 31 (2011) 1038–1061.
[9] X. Ye, A new discontinuous finite volume method for elliptic problems, SIAM J. Numer. Anal. 42 (2004) 1062–1072.
[10] D. Arnold, F. Brezzi, B. Cockburn, D. Marini, Unified analysis of discontinuous Galerkin methods for elliptic problems, SIAM J. Numer. Anal. 39 (2002) 1749–1779.
[11] B. Cockburn, G.E. Karniadakis, C.W. Shu (Eds.), The Discontinuous Galerkin Methods: Theory, Computation and Applications, in: Lec. Notes Comput. Sci. Engrg., vol. 11, Springer-Verlag, 2000.
[12] X. Ye, A discontinuous finite volume method for the Stokes problems, SIAM J. Numer. Anal. 44 (2006) 183–198.
[13] J. Liu, L. Mu, X. Ye, A comparative study of locally conservative numerical methods for Darcy's flows, Procedia Computer Science 4 (2011) 974–983.
[14] M. Crouzeix, P. Raviart, Conforming and nonconforming finite element methods for solving the stationary Stokes equations, RAIRO Anal. Numer. 3 (1973) 33–75.
[15] R.B. Kellog, On the Poisson equation with intersecting interfaces, Appl. Anal. 4 (1976) 101–129.
[16] R.E. Ewing, The Mathematics of Reservoir Simulation, SIAM, 1983.
[17] S.C. Brenner, L.R. Scott, The Mathematical Theory of Finite Element Methods, third ed., Springer, 2008.
[18] T. Gudi, A new error analysis for discontinuous finite element methods for linear elliptic problems, Math. Comp. 79 (2010) 2169–2189.
[19] J. Liu, L. Mu, X. Ye, L_2 error estimation for DGFEM for elliptic problems with low regularity, Appl. Math. Lett. (2012) (in press).
[20] T. Gudi, Some nonstandard error analysis of discontinuous Galerkin methods for elliptic problems, Calcolo 47 (2010) 239–261.
[21] T.P. Wihler, B. Riviére, Discontinuous Galerkin methods for second-order elliptic PDE with low-regularity solutions, J. Sci. Comput. 46 (2011) 151–165.
[22] R.A. Adams, J.J.F. Fournier, Sobolev Spaces, second ed., Academic Press, 2003.
[23] O. Karakashian, F. Pascal, A posteriori error estimates for a discontinuous Galerkin approximation of second order elliptic problems, SIAM J. Numer. Anal. 41 (2003) 2374–2399.
[24] J. Wang, Y. Wang, X. Ye, Unified a posteriori error estimator for finite element methods for the Stokes equations, SIAM J. Numer. Anal. (2011). Preprint (submitted for publication).
[25] X. Ye, A posterior error estimate for finite volume methods of the second order elliptic problem, Numer. Methods Partial Differential Equations 27 (2011) 1165–1178.
[26] J. Huang, S. Xi, On the finite volume elment method for general self-adjoint elliptic problems, SIAM J. Numer. Anal. 35 (1998) 1762–1774.
[27] R.A. DeVore, R.C. Sharpley, Besov spaces on domains in $\mathbb{R}^d$, Trans. Amer. Math. Soc. 335 (1993) 843–864.
[28] P. Morin, R.H. Nochetto, K.G. Siebert, Convergence of adaptive finite element methods, SIAM Rev. 44 (2002) 631–658.
[29] S. Sun, J. Liu, A locally conservative finite element method based on piecewise constant enrichment of the continuous Galerkin method, SIAM J. Sci. Comput. 31 (2009) 2528–2548.
[30] J. Liu, L. Mu, X. Ye, An adaptive discontinuous finite volume element method for elliptic problems, J. Comput. Appl. Math. 235 (2011) 5422–5431.